IMECE2015-53321

OPTIMAL POSITIONS FOR
MULTIPLE FLEXOELECTRIC ACTUATIONS ON BEAMS

B.L. Deng, H. Li, H.S. Tzou
StrucTronic Systems and Control Lab
School of Aeronautics and Astronautics, Zhejiang University
Hangzhou, Zhejiang 310027, P.R. China
Email: dengbolei@zju.edu.cn; Lhlihua@zju.edu.cn; hstzou@zju.edu.cn

ABSTRACT

Inhomogeneous electric field induces internal stress in flexoelectric materials, which is known as the *converse flexoelectric effect*. The atomic force microscope (AFM) probe can be applied to actuate the flexoelectric patch laminated on flexible structures and, in turn, induce structural vibrations. In this study, multiple actuators (i.e., combination of multiple AFM probes and flexoelectric patches) are used to suppress the vibration of an elastic cantilever beam. The displacement of the beam under control is obtained by superposition of a mechanical force induced part and an actuator induced part. The optimal actuator positions are selected when the minimal tip displacement of the cantilever beam is achieved. In case studies, only three actuators are used and only first three beam modes are considered. Under resonance conditions where only one mode participates, the optimal positions are obtained and they only depend on the relationship between actuation factor and actuator's position. The influence of the patch length is discussed, followed by the analysis of control voltages applied to actuators. When the control voltage is so small as to the induced displacement is far less than that induced by the mechanical force, the optimal actuation positions do not vary with the voltage magnitude; while when the voltage is relatively large the actuators keep adjusting their relative optimal positions with respect to the control voltage and the system becomes unstable. Furthermore, as long as the control voltage is relatively small below the stability threshold, the optimal positions do not change as the position where mechanical force placed along the beam. Under the small voltage condition, a smooth relationship between optimal positions and vibration frequency is obtained. There are four jump points of optimal positions and they are related to the tip displacement-actuator position curves under different frequencies. This study serves

as the foundation of flexoelectric vibration control with multiple AFM/flexoelectric actuators on flexible structures.

INTRODUCTION

Precision actuation and active vibration control based on smart materials has long been the focus of smart structures for years. According to the *converse flexoelectric effect*, where the electric field gradient induces stress inside the materials [1-3], flexoelectric materials can be applied to precision actuation and vibration control of flexible structures. The flexoelectricity has been, both theoretically [4-7] and experimentally [8-11], studied over the past decades. Recent years, flexoelectric sensors have been evaluated on various structures, i.e., cantilever beams [16], rings [12-14], cylindrical shells [15], etc. and its sensing effect was compared with that induced by piezoelectric materials [14]. Based on the cantilever beam model, theoretical flexoelectric signals were compared favorably with the experimental results [16]. Furthermore, the effect of static flexoelectric actuation by an atomic force microscope (AFM) probe was also evaluated [17].

Cantilever beam models are probably the most fundamental structure in engineering applications, such as wings, antennas, decks, robot arms, etc. Basic dynamics behaviors of cantilever beams have been thoroughly studied [18]. Comparing with single actuation and control, multiple actuators' control is probably more effective and versatile. This has been proved by pervious work on piezoelectric based multiple actuators [19-21] and studies on distributed sensing and actuating systems [22,23]. However, control effectiveness of multiple flexoelectric actuators has not been explored. In this study, multiple actuators are applied to control the vibration of an elastic cantilever beam, in which each actuator is consist of an AFM probe and a flexoelectric patch laminated on the beam surface. Considering the collaboration and interference among actuators,

their optimal positions are evaluated with regard to several system parameters, i.e., patch length, amplitude of control voltage, position of the external mechanical force and external excitation frequency. Theoretical derivations of the multi-AFM/flexoelectric patch model are presented first, followed by evaluations of those system parameters in case studies.

ACTUATION OF FLEXOELECTRIC PATCHES

A cantilever beam model, shown in **Fig.1**, is used to evaluate the optimal control positions of multiple AFM probes, where coordinates z and x respectively denote the transverse and longitudinal directions; L is the length; b is the width and h is the thickness of the cantilever beam. Assume that n flexoelectric patches of width L^a and n AFM probes of tip radius R are applied as actuators to control the beam vibration. Also, h^a is the thickness of the flexoelectric patches; x_i^* indicates the position of i-th probe and ϕ_i^a is the actuation voltage applied to the i-th probe.
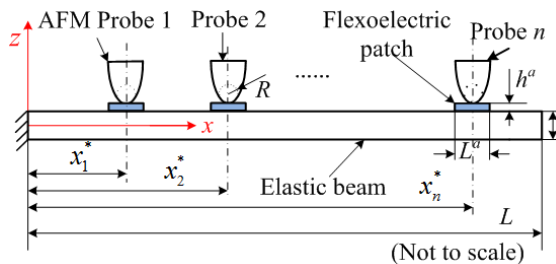
Figure 1. The cantilever beam model with multiple AFM control probes and flexoelectric patches.

Note that the beam thickness h is much thicker than that of the flexoelectric patch h^a and h^a is much greater than the AFM probe radius R, i.e., $R \ll h^a \ll h$. The flexoelectric patches need to be actuated by an inhomogeneous electric field, which is generated by AFM probes here. Recall that this study focuses on the optimal positions of these multi-probes, thus the position information is emphasized throughout. When actuation voltage ϕ_i^a is applied between the electrode of the i-th flexoelectric patch and i-th AFM probe, the transverse electric field between them can be defined by Abplanalp's approximate [24,25] as

$$E_z\left(x-x_i^*,z\right)=-\frac{\phi_i^a R\left(R+h/2+h^a-z\right)}{\left[\left(x-x_i^*\right)^2+\left(R+h/2+h^a-z\right)^2\right]^{\frac{3}{2}}}, \quad (1)$$

where E_z denotes the electric field strength in the transverse direction. According to the converse flexoelectric effect, the gradient of the electric field inside the flexoelectric material induces the stress and the normal stress in the longitudinal direction can be expressed as [17]

$$T_{xx}^a\left(x-x_i^*,z\right)=\pi_{12}\frac{\partial E_z}{\partial z}$$
$$=\frac{3\pi_{12}R\left(x-x_i^*\right)^2\phi_i^a}{\left[\left(x-x_i^*\right)^2+\left(R+h/2+h^a-z\right)^2\right]^{\frac{5}{2}}}-\frac{2\pi_{12}R\phi_i^a}{\left[\left(x-x_i^*\right)^2+\left(R+h/2+h^a-z\right)^2\right]^{\frac{3}{2}}}, \quad (2)$$

where T_{xx}^a denotes the longitudinal stress induced by the actuators. The converse flexoelectric coefficient π_{12} is defined as the ratio of longitudinal induced stress to the transverse gradient of transverse electric field. The membrane force of the flexoelectric patch can be calculated by integrating the stress through the patch thickness as

$$N_{xx}^a\left(x-x_i^*\right)=\int_{\frac{h}{2}}^{\frac{h}{2}+h^a}T_{xx}^a\left(x-x_i^*,z\right)dz$$
$$=\frac{\pi_{12}R\left(R+h^a\right)\phi_i^a}{\left[\left(x-x_i^*\right)^2+\left(R+h^a\right)^2\right]^{\frac{3}{2}}}-\frac{\pi_{12}R^2\phi_i^a}{\left[\left(x-x_i^*\right)^2+R^2\right]^{\frac{3}{2}}}, \quad (3)$$

where N_{xx}^a denotes the membrane control force in the longitudinal direction induced by the flexoelectric actuators. With the membrane force, one can obtain the bending control moment induced by the i-th actuator by multiplying the membrane force by a moment arm, i.e., the distance between the neutral layers of beam and patch, as

$$M_{xx}^a\left(x-x_i^*\right)=\frac{h+h^a}{2}\times N_{xx}^a\left(x-x_i^*\right)$$
$$=\frac{\pi_{12}R\left(h+h^a\right)\phi_i^a}{2}\left\{\frac{\left(R+h^a\right)}{\left[\left(x-x_i^*\right)^2+\left(R+h^a\right)^2\right]^{\frac{3}{2}}}-\frac{R}{\left[\left(x-x_i^*\right)^2+R^2\right]^{\frac{3}{2}}}\right\}, \quad (4)$$

where M_{xx}^a represents the control moment induced by the actuators. Note that the method used here to evaluate the control moment is an approximation. Considering the patch thickness is far less than the beam's thickness, this result is accurate enough. With the expressions of membrane force and control moment, the influence of the flexoelectric actuators on elastic beams can be analyzed next.

VIBRATION CONTROL WITH MULTIPLE ACTUATORS

Assume the mechanical excitation force F_3 and each actuator's control voltage ϕ_i^a are harmonic with the frequency ω, i.e., $F_3=F_3^*e^{j\omega t}$ and $\phi_i^a(t)=\phi_i^a e^{j\omega t}$. With harmonic

2

Copyright © 2015 by ASME

excitations, the steady-state response is also harmonic. Solving the equilibrium equation of elastic beam with the flexoelectric actuation, introducing the modal expansion method and giving the mode shape function of cantilever beams, one can determine the beam displacement induced by an external harmonic excitation force F_3 and harmonic flexoelectric actuations as [23]

$$u_3(x) = \sum_{k=1}^{\infty} \frac{U_{3k}(x)e^{j(\omega t - \varphi^*)}}{\omega_k^2 \sqrt{\left(1 - \frac{\omega^2}{\omega_k^2}\right)^2 + 4\zeta_k^2 \left(\frac{\omega}{\omega_k}\right)^2}} \left(\hat{F}_k^m + \hat{F}_k^a\right), \qquad (5)$$

where ω_k is the k-th natural frequency of the cantilever beam and ζ_k is the corresponding damping ratio which can be defined as $\zeta_k = c/(2\rho h \omega_k)$; U_{3k} is the cantilever beam's k-th mode shape function and can be written as [22]

$$U_{3k}(x) = C_k \Big[\cosh \lambda_k x - \cos \lambda_k x \\ - \frac{\cosh \lambda_k L + \cos \lambda_k L}{\sinh \lambda_k L + \sin \lambda_k L} \left(\sinh \lambda_k x - \sin \lambda_k x\right) \Big]; \qquad (6)$$

φ^* is the phase angle lagging behind the mechanical force expressed as

$$\varphi^* = \arctan \frac{2\zeta_k \left(\frac{\omega}{\omega_k}\right)}{1 - \frac{\omega^2}{\omega_k^2}}. \qquad (7)$$

$\hat{F}_k^m$ is the k-th modal force induced by the external mechanical excitation; $\hat{F}_k^a$ is the k-th modal force generated by all AFM probes and they can be expressed by introducing Love's control operator as [23]

$$\hat{F}_k^m = \frac{1}{\rho h N_k} \int_0^L F_3^* U_{3k}(x)\,dx, \qquad (8)$$

$$\hat{F}_k^a = \sum_{i=1}^{n} \hat{F}_{ik}^a = \sum_{i=1}^{n} \frac{1}{\rho h N_k} \int_{x_i^* - \frac{L^a}{2}}^{x_i^* + \frac{L^a}{2}} L_3^a\, U_{3k}(x)\,dx, \qquad (9)$$

where $N_k = \int_0^L U_{3k}^2\,dx$. Recall the external excitation is harmonic $F_3 = F_3^* e^{j\omega t}$. For the cantilever beam case, the Love's control operator can be reduced from the double-curvature shells as $L_3^a = \frac{\partial^2 M_{xxi}^a \left(x - x_i^*\right)}{\partial x^2}$ [23]; $\hat{F}_{ik}^a$ denotes the k-th modal force induced by the i-th actuator and the total effect of the probes can be regarded as the superposition of all probes' actuation

effect. The **modal actuation factor** of the i-th probe and k-th mode denotes the modal control force generated by the actuator with unit actuation voltage and it is defined as $A_k^a\left(x_i^*\right) = \hat{F}_{ki}^a / \phi_i^a$. The modal actuation factor of the i-th probe $A_k^a\left(x_i^*\right)$ contains the position information of the i-th probe influencing the beam vibration. Thus, the displacement of the cantilever beam with the control of n actuators can be expressed, with respect to their positions, as

$$u_3(x, x_1^*, x_2^*, \cdots, x_n^*) = \sum_{k=1}^{\infty} \frac{U_{3k}(x)e^{j(\omega t - \varphi^*)}}{\omega_k^2 \sqrt{\left(1 - \frac{\omega^2}{\omega_k^2}\right)^2 + 4\zeta_k^2 \left(\frac{\omega}{\omega_k}\right)^2}} \\ \times \left(\hat{F}_k^m + \sum_{i=1}^{n} \hat{A}_k^a\left(x_i^*\right) \phi_i^c \right), \qquad (10)$$

where the *modal actuation factor* can be written as

$$\hat{A}_k^a\left(x_i^*\right) = \frac{\hat{F}_{ik}^a}{\phi_i^a} \\ = \frac{1}{\phi_i^a \rho h N_k} \int_{x_i^* - \frac{L^a}{2}}^{x_i^* + \frac{L^a}{2}} \left(\frac{\partial^2 M_{xx}^a\left(x - x_i^*\right)}{\partial x^2} \right) U_{3k}(x)\,dx \\ = \frac{3\pi_{12} R \left(h + h^a\right)}{2\rho h N_k} \int_{x_i^* - \frac{L^a}{2}}^{x_i^* + \frac{L^a}{2}} \Bigg[\frac{4\left(R + h^a\right)}{\left[\left(x - x_i^*\right)^2 + \left(R + h^a\right)^2\right]^{\frac{5}{2}}} \\ \frac{5\left(R + h^a\right)^3}{\left[\left(x - x_i^*\right)^2 + \left(R + h^a\right)^2\right]^{\frac{7}{2}}} - \frac{4R}{\left[\left(x - x_i^*\right)^2 + R^2\right]^{\frac{5}{2}}} \\ + \frac{5R^3}{\left[\left(x - x_i^*\right)^2 + R^2\right]^{\frac{7}{2}}} \Bigg] U_{3k}(x)\,dx. \qquad (11)$$

Note that $L^a/2 \leqslant x_i^* \leqslant L - L^a/2$ because the flexoelectric patch has the length of L^a. Eq.(10) shows that the beam's displacement is related to the positions of n flexoelectric actuators. If a harmonic mechanical force excites the cantilever beam and n multiple actuators are used to control the harmonic vibration, the purpose of the vibration control is to minimize the tip displacement by adjusting probes' positions on the beam. In this study, only the actuator positions are analyzed, thus the voltages' amplitudes ϕ_i^a are set to a given value ϕ^a. The issue of searching optimal positions for multi-AFM probes

Copyright © 2015 by ASME

under given mechanical forces can be converted to an optimization mathematical model, i.e.,

$$\min\ u_3(L, x_1^*, x_2^*, \cdots, x_n^*)$$
$$s.t. \begin{cases} L^a/2 \le x_i^* \le L - L^a/2,\ \forall i \\ \left| x_i^* - x_j^* \right| \ge L^a,\ \forall i \ne j \end{cases} \quad (12)$$

To find the optimal positions for n probes to minimize the tip displacement, every possible combination of the AMF probes' positions should be tested. Then, the minimal tip displacement and the corresponding actuator positions are recorded. With the parameters listed in **Table 1**, the modal vibration control effects of the multiple flexoelectric actuators laminated on a cantilever beam are evaluated next.

Table 1. Parameters and properties of the beam model.

Properties	values
Beam length L, (m)	0.100
Beam width b, (m)	0.010
Beam thickness, h (m)	0.001
Young's modulus of beam, Y (N/m^2)	1.556×10^9
Flexoelectric patches thickness, h^a (μm)	50
Flexoelectric patches length, L^a (m)	0.010
AFM probe tip radius, R (nm)	50
Actuation voltage, ϕ (V)	33.33
External mechanical force, F_3(N)	0.01
Beam mass density, ρ (kg/m^3)	1100
Poisson's ratio, μ	0.3
Flexoelectric constant, π_{12} (μC/m)	100

CASE STUDIES

To demonstrate the multi-AMF probe actuations and their optimal positions, only three probes are used and only the first three modes of a cantilever beam are considered in case studies. Actuation characteristics of the multiple AFM probe control system are analyzed first, followed by the discussion of control effects and the corresponding optimal positions.

Case-1 Modal Optimal Actuator Positions

When actuation at resonance is considered, generally only one corresponding resonance mode is counted. Recall that the purpose of the vibration control here is to minimize the tip displacement of the cantilever beam. Thus, for the actuation case, the aim is to generate the maximal control force with multi-probe actuators to suppress the beam displacement and consequently cancel out the vibration induced by external mechanical excitations.

Since the first three beam modes, i.e. $k=1, 2, 3$, are evaluated here, the excitation frequencies applied to the AMF probes are respectively the three beam natural frequencies. Using the mathematical model presented in Eq.(12) gives the optimal positions for the three probes when the actuation voltage is harmonic at natural frequencies. These optimal AFM positions of mode 1, 2 and 3 are summarized in **Table 2**.

Table 2. Optimal actuator positions for three natural modes and their maximal actuator induced tip displacements.

Mode number	First actuator position (m)	Second actuator position (m)	Third actuator position (m)	Maximal induced tip displacement (μm)
1	0.005	0.015	0.025	365.14
2	0.005	0.048	0.058	52.862
3	0.031	0.066	0.076	18.178

The optimal actuator positions of three AMF probes, as listed in **Table 2**, are different for each natural mode. The free-end displacement under the k-th natural frequency can be deducted from the displacement expression of cantilever beam, i.e., Eq.(10), by setting $\omega = \omega_k$ and leaving only the k-th term, i.e.,

$$u_3(L, x_1^*, x_2^*, \cdots, x_n^*) = \frac{\phi^a U_{3k}(L) \sum_{i=1}^{n} \hat{A}_k^a\left(x_i^*\right)}{2\omega_k^2 \zeta_k}\, e^{j(\omega t - \varphi^*)}. \quad (13)$$

Eq.(13) indicates that for the resonance case the amplitude of the suppressed displacement is determined by the modal actuation factor $\hat{A}_k^a\left(x_i^*\right)$ of the corresponding mode. $\hat{A}_k^a\left(x_i^*\right)$ can be regarded as a function of the i-th probe's position x_i^* as the position varying to achieve the maximal displacement suppression. **Figure 3** shows the values of modal actuation factor for modes 1, 2, 3 as the probe's position varying from the fixed end ($x=0$) to the tip ($x=L$).

(a)

Copyright © 2015 by ASME
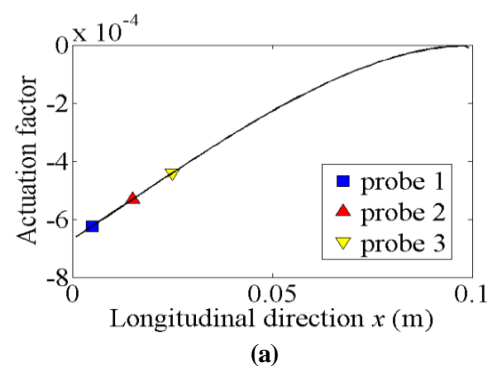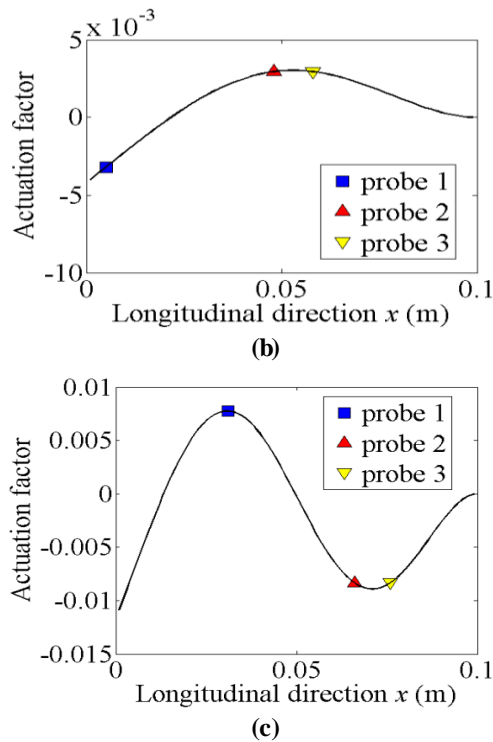
Figure 3. Actuation factor of mode (a) 1; (b) 2 and (c) 3 with the longitudinal coordinate.

The optimal actuator positions are labeled on the actuation factor curve in **Fig.3**. To achieve the maximal tip displacement suppression of the beam, the probes approach the positions where the value of actuation factor is relatively large while keeping a minimal distance between any two AFM probes to avoid stress concentrations, as shown in **Fig.3**. For mode 1, the actuation factor has only one peak at the fixed end, thus the probes cluster near the fixed end; for mode 2, two peaks exist and the probes arrange themselves to achieve the overall maximal effect; for mode 3, though at the fixed end the actuation factor reaches the maximal value, the actuator cannot be placed right at the fixed end but a space of half patch length $L^a/2$ away. Consequently, the probes go to the other two peaks of the actuation factor plot.

Note that the minimal distance between any two of the actuators is limited by the patches' length and permissible maximal actuation voltages. If such restriction is removed, the AMF probes would overlap each other at the point where actuation factor reaches its maximal value. For the cantilever beam case especially, as shown in **Fig.3**, such position is the fixed end of the cantilever beam. This concern of patches' length indicates that this parameter maybe one of the variables that influent the optimal positions of the actuators.

Case-2 Patch Length

Since probes/patches have to take up finite spaces and the previous discussion implies that the patch length could

influence the optimal positions of the actuators, influence of the patch length is evaluated in Case-2. The variation of the optimal positions with the flexoelectric patch length is analyzed here. Actuators' optimal positions of 1, 2 and 3 resonance modes are plotted in **Fig.4**.
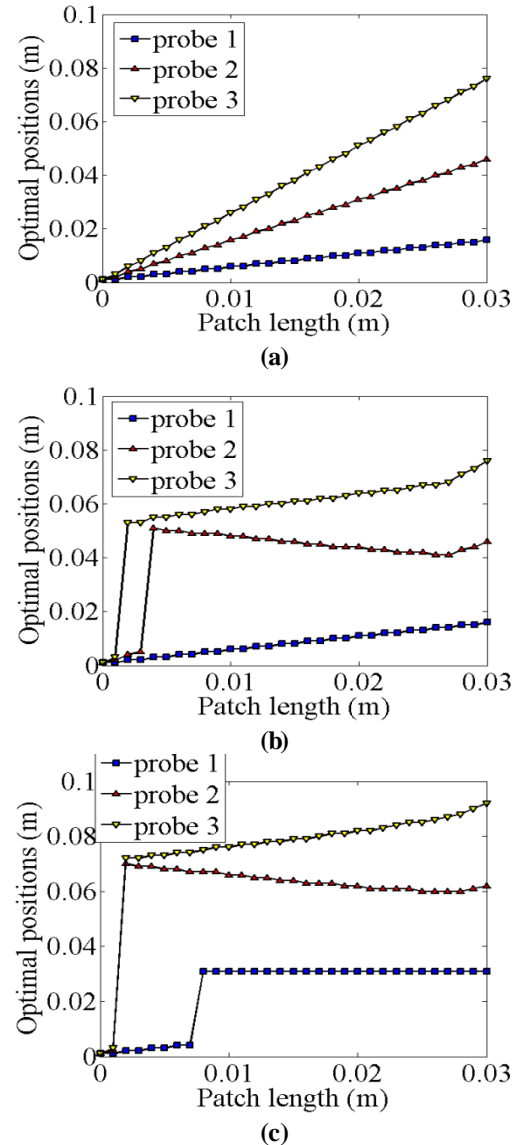
Figure 4. The relationship between optimal positions and patches length of (a) mode 1; (b) mode 2 and (c) mode 3.

In the beginning, all three AMF probes stay at the fixed end of the beam and then the probes move part from each other linearly as the flexoelectric patch length increases. For mode 1, as there isn't any peak in the actuation factor curve apart from the one at the fixed end, the actuators cluster near the fixed end as close as they are permitted; Where for modes 2 and 3, since there are other peaks existing in the actuation factor curve,

5

Copyright © 2015 by ASME

actuators would jump to other peaks to maintain the maximal tip displacement suppression as the patch enlarged.

Case-3 Actuation Voltages and Stability

The first two cases evaluated the actuation characteristics of the multi-probe actuation and control system and its modal actuation behaviors and position sensitivity. The purpose of the actuation is to induce the maximal tip displacement suppression of the beam to cancel out the displacement induced by external mechanical excitations. While if the maximal displacement suppression capability is too large as to outweigh the tip displacement induced by the mechanical force, the energy input to suppress the vibration is wasted and the system becomes unstable while the three probes keep looking for the optimal positions to maintain the minimal tip displacement. Such circumstance can be called instability of the system. According to the displacement expression i.e., Eq.(10), the control authority is related to the actuation voltage ϕ^a. When the actuation voltage is small enough, i.e., below the *stability threshold*, as to control induced displacement is far less than the mechanical force induced displacement, the instability absents. The optimal positions of the multi-AFM probes are the positions creating the maximal suppressions. As the actuation voltage increasing, the maximal tip displacement suppression grows bigger than the mechanical one. Probes may change their positions to avoid over-generating the maximal displacement and substitute with one position creating smaller tip displacement suppression.

To analyze this case, a harmonic point loading of 0.01N is applied at the center of the cantilever beam, i.e., x=0.05m. When the point loading excites the beam with the first natural frequency, the beam vibrates resonantly. Three flexoelectric actuators are placed on the beam and applied with resonance actuation voltages to minimize the tip displacement of cantilever beam. The variation of the optimal positions for three probes with the increase of actuation voltage's amplitude is plotted in **Fig.5**.

remain the same as the actuation voltage grows. While after a threshold point, the optimal positions start to distribute almost randomly or the system becomes unstable. As explained earlier, when the residue displacement reaches zero the probes have to change the positions to maintain the control effect and, thus, the system keeps looking for three optimal positions as observed in the figure. The relationship between the residual displacement and the actuation voltage is shown in **Fig.6**.
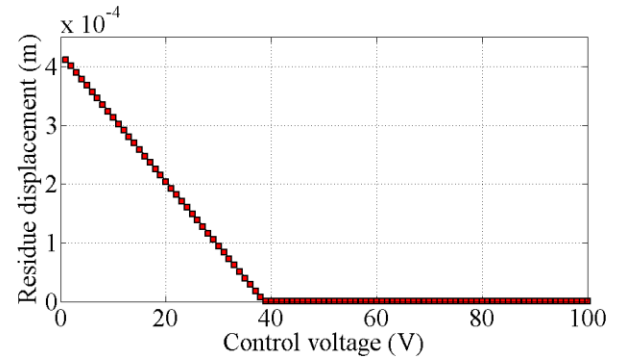
Figure 6. The residual tip displacement under the first mode resonance.

The point (i.e., the stability threshold) when the optimal positions of the actuator start to "randomly" distribute, coinciding with, as shown in **Fig.6,** the point when the residual tip displacement goes close to zero. Note that before the stability threshold the residual tip displacement decreases proportionally to the increasing of actuation voltages. Such phenomenon is reasonable according to the reduced displacement expression under resonance i.e., Eq.(13), when the actuator positions remain the same, the relationship between the tip displacement and actuation voltage is linear. Similar analysis is done on mode 2 and mode 3, when the mechanical force is harmonic with the 2nd and 3rd natural frequencies and the corresponding position/voltage results are plotted in **Fig.7**.

Figure 5. The optimal positions of three actuators under first mode resonance.

When the voltage amplitude is relatively small below the stability threshold, the optimal actuator positions, as predicted,

(a)

Copyright © 2015 by ASME

(b)

(c)

(d)
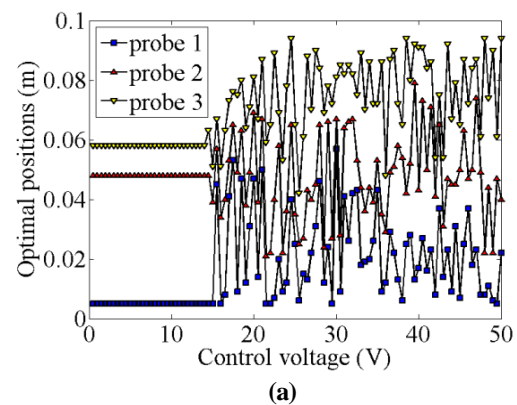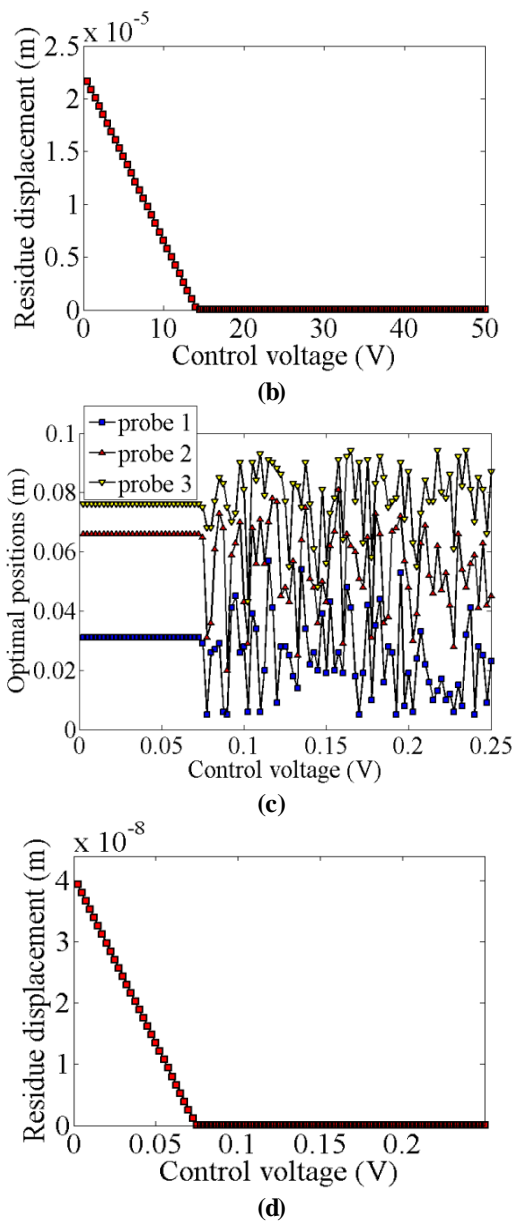
Figure 7. Optimal actuator positions of under (a) second mode (b) third mode resonances; the residual tip displacement of (c) second mode (d) third mode.

When actuation voltage is relatively small below the stability threshold, the actuators' control ability is weak. Thus, the three AMF probes works together to resist the vibration induced by the mechanical excitation. At this moment, the optimal actuator positions coincide with the optimal positions for the maximal displacement suppression discussed in Case-1. While as the actuation voltage becomes larger than necessary, the actuations are so strong as to interference with each other. Under this circumstance, more than suppressing the tip displacement induce by the mechanical force, they have to adjust their relative positions to maintain the control effect and,

thus, the system becomes unstable. Focusing on the stable part, characteristics of the actuators under small actuation voltage below the stability threshold are studied in the following part. Another reason for focusing on small voltage is that too large voltage applying on the flexoelectric patch could induce serious stress concentration possibly even breaking the flexoelectric material [17].

Case-4 Position of Mechanical Point Force

The actuation voltage, as discussed in the third case, would not influence the optimal actuator positions as long as it is relatively small as compared with the mechanical counterpart. The influence of the position of mechanical point loading is evaluated here. The actuation voltage used here is 0.1V, and a 0.01N point loading excites the beam at various positions from the fixed end to the tip. Note that the actuation voltage chosen here remains small enough to ensure the absence of instability. Again, the excitation frequency of the mechanical force and actuation voltage is set to be the first, second and third natural frequencies. The optimal actuator positions as the point loading moving on the beam are plotted in **Fig.8**.

(a)

(b)

7

Copyright © 2015 by ASME

(c)
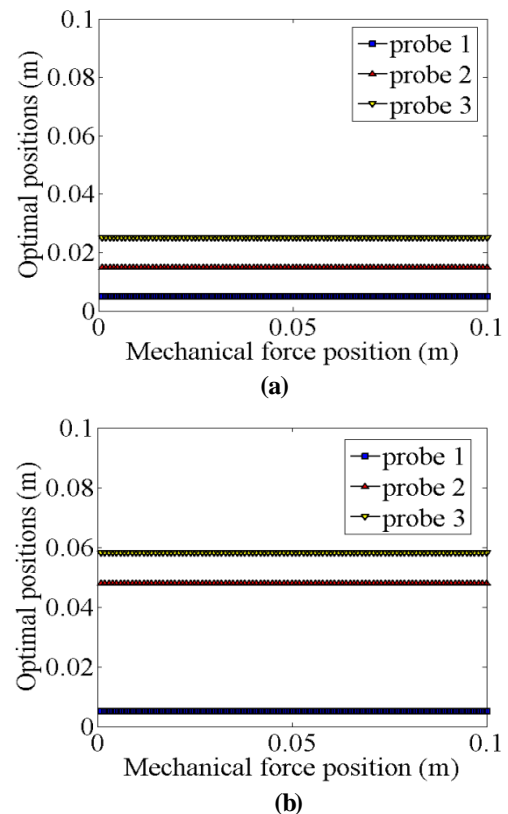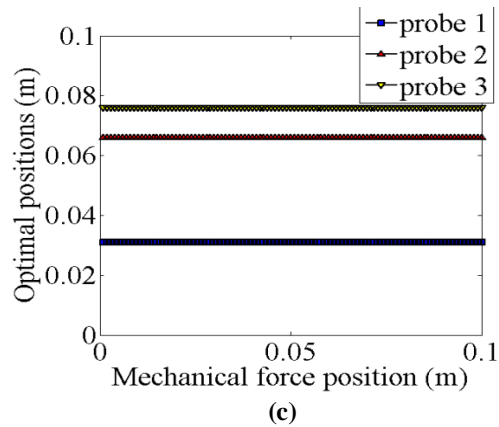
Figure 8. Optimal actuator positions under different point loading positions of (a) first mode; (b) second mode; (c) third mode.

As shown in **Fig.8**, the optimal actuator positions remain unchanged as the point loading moving from $x=0$ to $x=L$. In other words, the positions of the mechanical force do not influence the optimal AFM actuator positions. The displacement induced by the point loading is far larger than the tip displacement suppression induced by the flexoelectric actuators. Thus, the actuators' optimal positions are those which generate the maximal tip displacement suppression. Recall that Case-1 reveals the optimal actuator positions of modes 1, 2 and 3 in **Fig.8** are identical to those listed in **Table 2**. Note that although when voltage is relatively small the optimal positions are independent from the location of mechanical excitations, the optimal positions for modes 1, 2, 3 are different from each other. Thus, the frequency of the mechanical force seems the only external variable that influences the optimal actuator positions. The relationship between them is discussed in the next case.

Case-5 Excitation Frequency of Mechanical Force

In the beginning, the hypothesis was that the optimal actuator positions on the cantilever beam could be influenced by the actuation voltage, the position of mechanical force and the excitation frequency. While as the voltage induced displacement is relatively small as compared with that induced by the mechanical force, as discussed in Case-3 and Case-4, the optimal positions remain unchanged as the actuation voltage or position of point loading varying. Under this circumstance, the excitation frequency becomes the only variable that influences the optimal positions and this is evaluated in this case. The actuation voltage is set to a relatively small value 0.1V and point loading of 0.01N applied at the center ($x=0.05$m) of the cantilever beam. Previous studies suggest that neither changing the magnitude of actuation voltage and point loading nor moving the excitation position of point loading could change the optimal actuator positions, as long as the actuation effect is smaller than the mechanical induced vibration. This assumption is reasonable considering that the voltage applied on the probe

must be limited to avoid the stress concentration. The frequency becomes the only variable here and the relationship between the optimal positions and the excitation frequency from 0Hz to 400Hz is plotted in **Fig.9**.
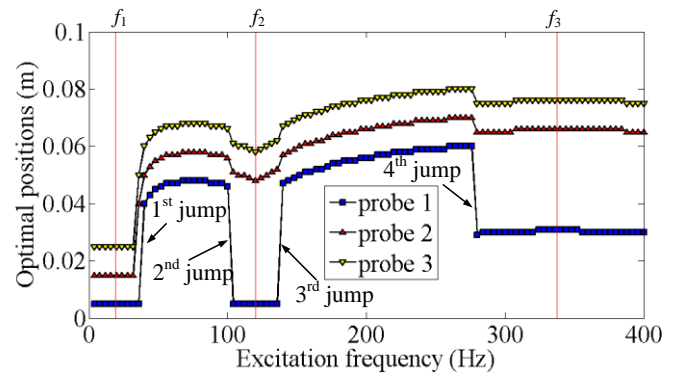
Figure 9. The variation of optimal actuator positions with excitation frequency.

The three vertical lines, shown in **Fig.9**, indicate the first, second and third natural frequencies. The optimal positions at these three points are identical to the optimal positions under resonance actuations presented in Case-1. The actuator positions on the cantilever beam under various excitation frequencies are plotted in **Fig.9**. Note that at four jump points, i.e., 36Hz, 104Hz, 140Hz and 312Hz, the optimal positions jump from one set to another and these detailed transitions are discussed and plotted next. Note that the actuation voltage used here is relatively small, thus the optimal positions for multi-actuators are equal to those inducing the maximal controllable displacement for actuators, which can be obtain by the tip displacement, i.e., Eq.(10), as

$$u_3(L) = \phi^c \sum_{k=1}^{\infty} \frac{U_{3k}(L)\mathrm{e}^{j(\omega t - \varphi^*)}\sum_{i=1}^{n} \hat{A}_k^a\left(x_i^*\right)}{\omega_k^2 \sqrt{\left(1 - \dfrac{\omega^2}{\omega_k^2}\right)^2 + 4\zeta_k^2\left(\dfrac{\omega}{\omega_k}\right)^2}} . \tag{14}$$

When the tip of the beam is considered, Eq.(14) reveals that the magnitude of the tip displacement can be regarded as a function of the actuators' positions x_i^* embedded in the actuation factor $\hat{A}_k^a\left(x_i^*\right)$ and the excitation frequency ω. Detailed amplitudes of beam tip vibration are plotted in **Fig.10** with frequencies near four jump points, where only three intermediate frequencies are marked. When the frequency is relatively low, i.e., near the first natural frequency, the fixed end, as shown in **Fig.10(a)**, represents better actuation positions for actuators. Thus, the actuators cluster near the fixed end as illustrated in **Fig.9**.

8

Copyright © 2015 by ASME

(a)

(b)

(c)

(d)
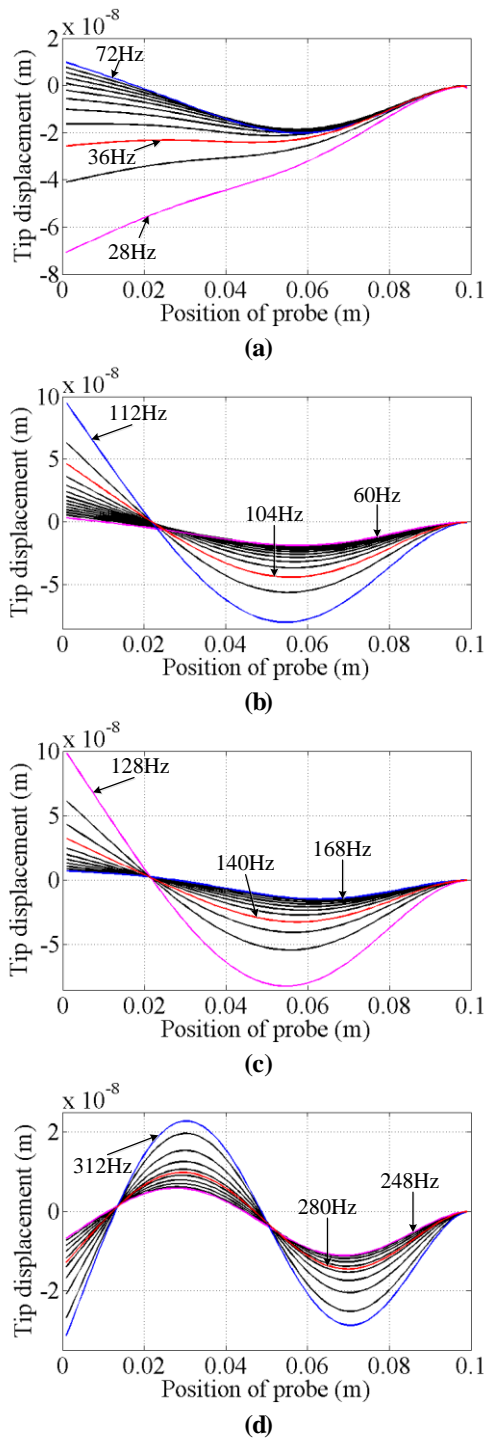
Figure 10. Transitions of beam tip displacements with probe positions under different frequencies near (a) first, (b) second, (c) third and (d) fourth jump points.

As the frequency moves up, the fixed end is no longer the best positions for all three actuators. When the frequency is equal of 36Hz, the region near the middle of the beam becomes better than the fixed end. Thus, three actuators jump from the fixed end to the middle of the beam as shown in **Fig.9** at the first jump point. As the frequency keep increasing towards the second natural frequency, as shown in **Fig.10(b)**, the figure begins to look like the actuation factor curve under the second natural frequency as represented by **Fig.3(b)**. The fixed end at this frequency becomes more favorable to induce large displacement, thus one of the actuator jumps to the fixed at 104 Hz which is the second jump point. The same behavior can explain the third and fourth jump points.

To obtain the maximal displacement suppression, the actuators are always searching for the positions where the best actuation effect is achieved. While the so called best position is only a function of excitation frequency, thus **Fig. 9** illustrates the trend of optimal positions for the AFM probe actuators. Note that although the case studies here limit the number of actuators to three, however, the theory can be applied to arbitrary number of probes as long as they can be placed on the cantilever beam.

CONCLUSION

Based on the *converse flexoelectric effect*, the flexoelectric materials, under the electric field gradient induced by AFM probes, can be used as actuators to control the structural vibrations. In this study, multiple flexoelectric actuators were used to obtain better control effects of the cantilever beam, while the actuator positions must be carefully chosen to guarantee the maximal tip displacement suppression. Thus, the optimal positions of the actuators (i.e., AFM probes and flexoelectric patches) were defined to minimize the tip displacement when subjected to external excitations. The optimal positions were obtained by testing every possible arrangement of the actuator's positions and selecting the best combinations. To suppress the vibration induced by the external mechanical force, the target of introducing the maximal displacement suppression induced by the multiple actuators was pursued. For the resonance case, this target is identical as maximizing the summation of the actuation factor of each actuator and the actuation factor curve was given to demonstrate where the optimal positions are under resonance conditions. The patches' size, i.e., length, also influences the optimal positions of the actuators. As the patches' length increasing, the probes are forced to separate from each other, which leads to their possible positions are limited to avoid overlapping and stress concentrations. If the length is infinitesimal, the actuators all clustered to the fixed end where the actuation factors maximize for every natural mode.

Furthermore, the amplitude of control voltage does not influence the optimal actuator positions when the control voltage is relatively small under the stability threshold. While as the control voltage enhanced, the control authority, i.e., the maximal displacement suppression, becomes stronger than the original vibration and thus unstable phenomenon occurs. The actuators have to adjust their relative positions continuously

9

Copyright © 2015 by ASME

according to the amplitude of control voltage to keep the overall tip displacement minimal. When the control voltage goes beyond the threshold, the three actuators constantly regulate themselves and the system becomes unstable between the optimal positions and the control voltage. In addition, as long as the control voltage is relatively small under the stability threshold, changing the excitation position do not influent the optimal actuator positions. Finally, under the small control voltage assumption, the optimal actuator positions change with respect to the excitation frequency, which are smooth near the resonance frequencies and show four salient jumps during modal transitions with different mode shapes. Multiple flexoelectric actuators, thus, can be used to control the vibration of cantilever beams, whose optimal actuator positions can be determined as long as excitation frequency is given. This multi-AFM probe actuation and control methodology can be further extended to control of other flexible structures.

ACKNOWLEDGEMENTS

REFERENCES

[1] Kogan, S. M., 1964, "Piezoelectric Effect During Inhomogeneous Deformation and Acoustic Scattering of Carriers in Crystals," Soviet Physics-Solid State, 5(10), pp.2069-2070.

[2] Mindlin, R. D., and Eshel, N. N., 1968, "On Fisrst Strain-gradient Theories in Linear Elasticity," International Journal of Solids and Structures, 4(1), pp.109-124.

[3] Todorov, A. T., Petrov, A. G., and Fendler, J. H., 1994, "First Observation of the Converse Flexoelectric Effect in Bilayer Lipid Membranes," The Journal of Chemical Physics, 98(12), pp.3076-3079.

[4] Mindlin, R. D., 1969, "Continuum and Lattice Theories of Influence of Electromechanical Coupling on Capacitance of Thin Dielectric Films," International Journal of Solids and Structures, 5(11), pp.1197-1208.

[5] Tagantsev, A. K., 1986, "Piezoelectricity and Flexoelectricity in Crystalline Dielectrics," Physical Review B, 34(8), pp.5883-5889.

[6] Sahin, E., and Dost, S., 1988, "A Strain-Gradients Theory of Elastic Dielectrics with Spatial-Dispersion," International Journal of Engineering Science, 26(12), pp.1231-1245.

[7] Cross, L. E., 2006, "Flexoelectric Effects: Charge Separation in Insulating Solids Subjected to Elastic Strain Gradients," Journal of Materials Science, 41(1), pp.53-63.

[8] Baskaran, S., He, X., and Chen, Q., 2011, "Experimental Studies on the Direct Flexoelectric Effect in α-phase Polyvinylidene Fluoride Films," Applied Physics Letters, 98(24), p.242901.

[9] Agronin, A., Molotskii, M., Rosenwaks, Y., Rosenman, G., Rodriguez, B. J., Kigon, A. I., and Gruverman, A., 2006, "Dynamics of Ferroelectric Domain Growth in the Field of Atomic Force Microscope," Journal of Applied Physics, 99(10), p.104102.

[10] Fu, J. Y., Zhu, W., Li, N., Cross, L. E., 2006, "Experimental Studies of the Converse Flexoelectric Effect Induced by Inhomogeneous Electric Field in a Barium Strontium Titanate Composition," Journal of Applied Physics, 100(2), pp.024112.

[11] Zubko, P., Catalan, G., Buckley, A., Welche, P. R. L., and Scott, J. F., 2007, "Strain-Gradient-Induced Polarization in SrTiO3 Single Crystals," Physical Review Letters, 99, p.167601.

[12] Hu, S. D., Li, H., and Tzou, H. S., 2013, "Flexoelectric Responses of Circular Rings," Journal of Vibration and Acoustics, 135(2), p.021003.

[13] Hu, S. D., Tzou, H. S., 2010, "Signal Analysis of Flexoelectric Transducers on Rings," Proceedings of the 2010 Symposium on Piezoelectricity, Acoustic waves, and Device Applications, SPAWDA10, pp.106-111.

[14] Hu, S. D., Li, H., and Tzou, H. S., 2014, "Comparison of Flexoelectric and Piezoelectric Dynamic Signal Responses on Flexible Rings," Journal of Intelligent Material Systems and Structures, 25(7), pp.832-844.

[15] Rao, Z., Hu, S. D., Tzou, H. S., 2011, "Diagonal Flexoelectric Sensor on Cylindrical Shell Substructure," Proceedings of the 2011 Symposium on Piezoelectricity, Acoustic waves, and Device Applications, SPAWDA10, pp.106-111.

[16] Hu, S.D., Li, H., and Tzou, H.S., 2011, "Static Nano-Control of Cantilever Beams Using the Inverse Flexoelectric Effect," Proceedings of the ASME 2011 IMECE, IMECE2011-65123, pp.463-470.

[17] Hu, S. D., Li, H., and Tzou, H. S., 2011, "Static Nano-Control of Cantilever Beams Using the Inverse Flexoelectric Effect," Proceedings of the ASME 2011 IMECE, IMECE2011-65123, pp.463-470.

[18] Sodel, W.,1993, Vibrations of Shells and Plates, Dekker, New York.

[19] Yan, Y. J., and Yam, L. H., 2002, "Optimal Design of Number and Locations of Actuators in Active Vibration Control of a Space Truss," Smart Materials and Structures, 11(4), pp.496-503.

[20] Clark, R. L., Fuller, C. R., 1992, "Experiments on Active Control of Structurally Radiated Sound Using Multiple Piezoceramic Actuators," The Journal of the Acoustical Society, 11(4), pp.496-503.

[21] Caruso, G., Galeani, S., and Menini, L., 2003, "Active Vibration Control of an Elastic Plate Using Multiple Piezoelectric Sensors and Actuators," Simulation Modelling Practice and Theory, 11(5-6), pp,403-419.

[22] Bailey, T., and Hubbard, J. E., 1985, "Distributed piezoelectric-polymer active vibration control of a cantilever beam", Journal of Guidance, Control, and Dynamics, 8(5), pp. 605-611.

[23] Tzou, H. S., 1993, Piezoelectric Shells: Distributed Sensing & Control, Kluwer Academic Publishers, Dordrecht, Boston, London.

[24] Abplanalp, M., 2001, Piezoresponse Scanning Force Microscopy of Ferroelectric Domains, Ph.D. Dissertation, Swiss Federal Institute of Technology, Zürich.

[25] Agronin, A., Molotskii, M., Rosenwaks, Y., Rosenman, G., Rodriguez, B. J., Kingon, A. I., and Gruverman, A., 2006, "Dynamics of Ferroelectric Domain Growth in the Field of Atomic Force Microscope," Journal of Applied Physics, 99(10), p.104102.

Copyright © 2015 by ASME